

Terahertz photo-Hall measurements of carrier mobility in GaAs and InP

J. N. Heyman,^{a)} D. Bell, and T. Khumalo

Department of Physics and Astronomy, Macalester College, St. Paul, Minnesota 55105

(Received 18 November 2005; accepted 30 January 2006; published online 18 April 2006)

We have developed a sensitive ultrafast technique for measuring the mobility of photocarriers in semiconductors. High-resistivity samples are photoexcited with a femtosecond laser, and carrier mobilities are determined by polarization-sensitive terahertz emission measurements in a magnetic field. Measurements on a semi-insulating GaAs sample at $T=280$ K yielded $\mu_e = 4400 \pm 600$ cm²/V s and $\mu_h = 850 \pm 400$ cm²/V s within 0.5 ps of excitation with $\lambda=800$ nm radiation. In GaAs, this zero-background technique requires ~ 10 pJ/pulse photoexcitation and can be easily implemented with an unamplified Ti:S laser oscillator. © 2006 American Institute of Physics. [DOI: 10.1063/1.2187520]

Technological progress in high-speed electronics and optoelectronics makes it important to understand conduction in electronic materials on picosecond time scales. Ultrafast optical techniques such as time-resolved luminescence have been widely used to probe carrier dynamics in materials with subpicosecond time resolution.¹ These techniques primarily probe interband electronic transitions, and may yield the distribution of carriers in the conduction and valance bands following excitation. In contrast, ultrafast terahertz techniques directly probe carrier transport and measure conductivity or mobility.

A number of scientists have used terahertz (THz) time domain spectroscopy to probe the conductivity of semiconductors as a function of frequency.²⁻⁴ This technique probes extrinsic carriers at equilibrium conditions and is not time resolved. Mittelman *et al.*⁵ developed a THz noncontact Hall effect measurement in which the equilibrium extrinsic carrier concentration and mobility are determined by analyzing the magnetic-field dependence of the polarization of THz pulses that are transmitted through a sample or reflected from its surface with a lateral resolution ~ 0.25 mm, set by the focal spot size of the THz beam.

Time-resolved terahertz spectroscopy (TRTS) (Refs. 6–14) can be used to determine the time dependence of the conductivity of photocarriers in materials. Here, a near-IR or visible pump pulse excites a population of photocarriers at the surface of a semiconductor, and the transmission of a THz probe pulse through the photoexcited region is measured as a function of the delay between pump and probe pulses. TRTS requires an intense pump pulse in order to produce a measurable change in the THz optical properties of the sample, and these measurements are generally carried out with amplified Ti:sapphire laser systems. As in THz noncontact Hall measurements, the spatial resolution of TRTS is limited by the focal spot size of the THz beam.

Several groups have used THz emission¹⁵⁻¹⁷ measurements to study carrier scattering in semiconductors. In general, very high temporal resolution is required ($\Delta\tau < 20$ fs) to fully explore the dynamics, which for experimental reasons (use of very thin electro-optic detectors) limits the sensitivity of these measurements.

We have developed a THz version of the photo-Hall effect measurement. We applied an electric field parallel to the surface of the photoconductor by applying a voltage between metallic contacts. The region between the contacts is photoexcited with a femtosecond laser pulse at normal incidence (Faraday geometry), producing THz radiation. We apply a magnetic field normal to the semiconductor surface and measure the polarization of the emitted THz as a function of the magnetic field. At zero magnetic field, the emitted radiation is polarized parallel to the applied E field.¹⁸ For nonzero B fields, we also observe a THz signal polarized perpendicular to the E field. These two signals are used to determine the mobility of the photoexcited electrons and holes approximately 0.5 ps after photoexcitation.

A simple model describes how the terahertz photo-Hall technique works. We assume an effective relaxation time τ_i for each carrier type. Neglecting interaction between carriers, the equation of motion of the i th species of photocarrier is then given by

$$\frac{\partial^2 \mathbf{r}_i}{\partial t^2} = \frac{q_i}{m_i} (\mathbf{E} + \mathbf{v}_i \times \mathbf{B}) - \mathbf{v}_i / \tau_i. \quad (1)$$

We solve the equations of motion under the initial conditions $\mathbf{v}_i=0$ at $t=0$ to obtain the carrier trajectories, and use these to simulate the THz signal. The predicted magnetic-field dependence of the signal becomes simple in the limit that the carrier scattering time is much shorter than the temporal resolution of the THz system. In our system this is satisfied for scattering times $t \leq 10^{-13}$ s, which describes most semiconductors near room temperature. In this limit, the magnetic-field dependence of the amplitude of the THz signal polarized parallel and perpendicular to E becomes

$$\begin{aligned} S_{\parallel} &\propto \left\langle \frac{\partial^2 p_{\parallel}}{\partial t^2} \right\rangle \propto \frac{\mu_e}{1 + \mu_e^2 B^2} + \frac{\mu_h}{1 + \mu_h^2 B^2}, \\ S_{\perp} &\propto \left\langle \frac{\partial^2 p_{\perp}}{\partial t^2} \right\rangle \propto \frac{\mu_e^2 B}{1 + \mu_e^2 B^2} - \frac{\mu_h^2 B}{1 + \mu_h^2 B^2}. \end{aligned} \quad (2)$$

We have assumed an equal population of electrons and holes, and a single effective mobility for each species. These formulas exhibit the same dependence on the magnetic field as the steady-state photocurrent.¹⁹ However, the electron and

^{a)}Electronic mail: heyman@macalester.edu

hole mobilities reflect the conditions immediately after photoexcitation.

The THz photo-Hall technique we have developed has some unique capabilities. It is a zero-background technique in which the sample itself is the radiation source. For this reason measurements can be carried out at much lower excitation densities than those required for TRTS, using only a simple Ti:sapphire oscillator system. In GaAs, mobility measurements can be performed using optical excitation of only $\sim 10^{-11}$ J/pulse. The temporal resolution of the measurement system need not be shorter than the carrier scattering times. In addition, this technique directly measures the Hall mobility of photocarriers, rather than the conductivity. Finally, the spatial resolution of this technique is set by the focal spot size of a near-IR beam, so that it may form the basis of an imaging system with ~ 1 μm lateral resolution. We also note some limitations. As proposed here, the technique can only be applied to high-resistivity materials. In addition, we have not yet developed a pump-probe version of this technique suitable for measuring the evolution of the mobility following excitation. However, in certain cases it is possible to extract the carrier dynamics from analysis of the THz wave form.

We have tested our technique by investigating bulk semi-insulating GaAs and InP:Fe(100) wafers purchased from WaferTech Ltd. Aluminum contacts were evaporated on the surface of the samples. We investigated contact spacings of 0.4 mm and 160 μm . Each sample was mounted onto a silicon hyperhemispheric lens, and then loaded into an Oxford Instruments magneto-optical cryostat for THz emission measurements.

The samples were excited with a femtosecond mode-locked Ti-sapphire laser and THz emission was observed when a bias voltage was applied across the sample contacts. The pump beam was normally incident on the sample surface. THz radiation was collected in the pseudotransmission geometry and focused onto a 2 mm thick $\langle 110 \rangle$ ZnTe electro-optic detector using two off-axis parabolic mirrors. In our system, the laser pulse width was $\Delta t = 10$ fs, the center wavelength was $\lambda = 800$ nm, the spectral bandwidth was $\Delta\lambda = 110$ nm, and the pulse energy was 1.5 nJ/pulse at the sample (see Fig. 1). The laser spot size at the sample was ~ 0.2 mm diam. The laser could also be frequency doubled using a 0.5 mm BBO crystal, yielding 0.3 nJ pulses with a center wavelength of 400 nm. Bias voltages in the range 40–60 V were used. The sign of the voltage was modulated at 2.5 kHz and the signal was measured with a lock-in amplifier. The THz beam path was purged with dry air to suppress absorption of the THz radiation by water vapor. In these measurements we have optimized our system for sensitivity rather than for THz bandwidth: the hyperhemispheric lens and the 2 mm thick ZnTe detector reduced the bandwidth of our system to ~ 1.5 THz.

We used the polarization sensitivity of the electro-optic effect to independently measure the THz emission polarized parallel and perpendicularly to the applied electric field at the sample. This was done by orienting the $\langle 110 \rangle$ ZnTe detector crystal so that the desired polarization was parallel to the $[1, -1, 0]$ crystallographic direction. In this case the unwanted polarization was parallel to the $[0, 0, 1]$ direction, and produced no signal.

We have recorded the amplitude versus the time of the THz emission from our samples as a function of temperature

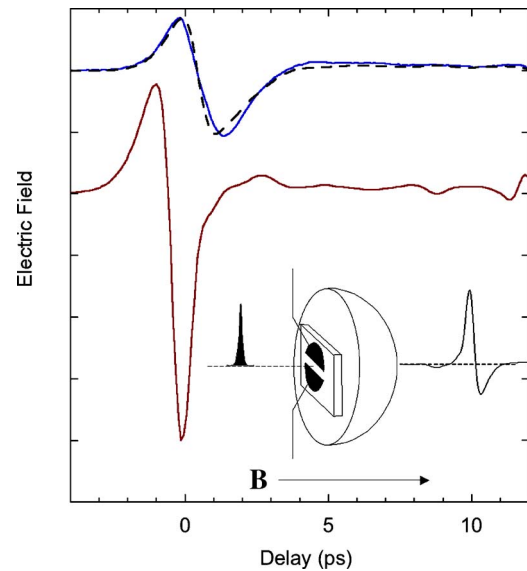


FIG. 1. THz emission from Si-GaAs at $B=0$ and $T=180$ K using $\lambda = 800$ nm femtosecond pump laser pulses (lower trace) and 400 nm pulses (upper trace). The dashed line is a fit to our model. Inset: experimental geometry.

and magnetic field. When the emitters are excited with 800 nm laser pulses, we find that the amplitude of the THz signal is strongly dependent on the magnetic field, but that the *shape* of the THz wave form is only weakly field dependent. Likewise, we find that the wave-form shape is nearly temperature independent for sample temperatures above 100 K. This suggests that the carrier scattering rate is larger than the bandwidth of our optical system, so that the shape of these THz wave forms is determined by the instrument response function of our system.

THz wave forms obtained using 400 nm excitation in GaAs are temporally broader than those obtained using 800 nm excitation, demonstrating that our optical system does resolve the time dependence of the conductivity in this case. In GaAs, excitation with 400 nm radiation produces hot carriers that rapidly scatter into the low-mobility L and X valleys of the conduction band. Following excitation, the electrons cool, and transfer back into the Γ valley. We are able to fit the 400 nm pump THz wave form by assuming that the carrier density in the Γ valley is negligible immediately after photoexcitation and exponentially approaches an equilibrium value, with $\sigma(t) = n_{\Gamma}(t)\mu_{\Gamma}e$, where $n_{\Gamma}(t) = n_0(1 - e^{-t/\tau})$, and we approximate the carrier mobility in the Γ valley as constant. The calculated emission based on this model is then convolved with the impulse response function of our system to get a simulated THz wave form. Fitting this response to our data yields a relaxation time into the Γ valley of 1.2 ± 0.3 ps, compared to relaxation times of 0.7–2.0 ps obtained by TRTS.⁷ The relative amplitude of wave forms obtained with 400 nm excitation to those obtained with 800 nm excitation is $\sim 1:4$, after correction is made for the photon flux from the pump laser. This is of the same order as the ratio of mobilities listed in Table I.

Further measurements were made by monitoring the peak THz signal in each wave form as a function of the magnetic field. Figures 2(a) and 2(c) show the THz signal amplitude as a function of the magnetic field in Si-GaAs photoexcited with near-band-gap radiation at $T=280$ and 180 K. The amplitude of the THz signal polarized parallel to

TABLE I. Electron and hole mobilities determined from our measurements for our semi-insulating GaAs and InP samples. The dc Hall mobilities were measured at low frequencies under ambient conditions.

| | λ pump (nm) | μ_e (cm ² /V s) (THz) | μ_h (cm ² /V s) (THz) | μ_{Hall} (cm ² /V s) dc |
|--------------|------------------------|---|---|--|
| GaAs (280 K) | 800 | 4400±600 | 850±400 | 6950 |
| InP (280 K) | 800 | 1475±250 | 575±300 | 2350 |
| GaAs (180 K) | 800 | 7200±1000 | 1150±600 | |
| GaAs (180 K) | 400 | 2750±400 | 1200±400 | |

the applied bias reaches a maximum at zero field and decreases with increasing field. The THz signal polarized perpendicular to the applied bias changes sign near zero magnetic field, increases with magnetic field to a maximum value at $B \sim 1.5$ T, and then decreases as the field is increased further. The magnetic-field dependence of the THz signal in InP:Fe [Fig. 2(b)] is qualitatively similar to that in GaAs, although the amplitude varies more slowly with the field. In this sample the THz signal polarized perpendicular to the bias does not reach a maximum below 5 T. We also obtain qualitatively similar results for SI-GaAs excited with 400 nm radiation. In this case the perpendicular component of the THz signal reaches a maximum value near $B=2$ T, and then remains approximately constant.

We obtain excellent fits to the data with our model. Three fitting parameters are used to fit the magnetic-field dependence of the THz signal amplitude both parallel and perpendicular to the bias: the electron and hole mobilities and a single overall scaling factor. The mobilities determined from these fits are shown in Table I. We note that the fits are not strongly dependent on the effective hole mobility, and so this parameter is only determined within $\sim 50\%$. The THz electron mobilities for our GaAs and InP samples at 280 K are $\sim 60\%$ of the room-temperature dc Hall mobilities for these wafers as measured by the vendor. Our lower measured values may reflect the high photocarrier density, which we estimate to be $\sim 10^{17}$ cm⁻³. We note that the room temperature mobility of *n*-GaAs-doped $\sim 10^{17}$ cm⁻³ is also $\sim 60\%$ that of lightly doped material,²⁰ and that Beard *et al.*²¹ observe a decrease in mobility for photocarrier densities of this order in GaAs at 77 K. We did not investigate the dependence of mobility on photocarrier density in this letter. In the case of THz emission using a 400 nm pump, simulated wave forms were generated using a time-dependent carrier population in the Γ valley as described above, a Γ valley electron mobility and a hole mobility. The maxima of the simulated wave forms were then plotted as a function of the magnetic field. The low electron mobility reflects the hot carrier conditions in the Γ valley within a few picoseconds of photoexcitation.

In conclusion, we have developed an ultrafast technique for measuring carrier mobilities in photoconductors based on THz emission measurements performed in a magnetic field. This is a sensitive zero-background technique, which can be implemented with an unamplified femtosecond Ti:S laser. The bandwidth of the THz system does not need to exceed the scattering rate to obtain carrier mobilities. We have used this technique to examine photoconductivity in SI-GaAs and InP:Fe, and obtain electron mobilities $\sim 60\%$ of dc Hall mobilities.

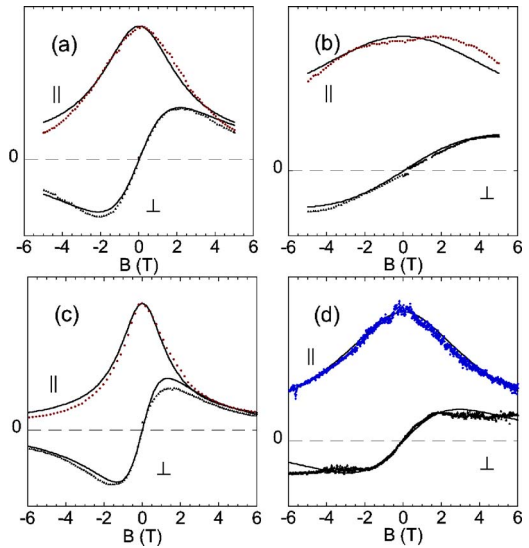


FIG. 2. THz signal amplitude vs magnetic field for THz polarizations parallel and perpendicular to the bias electric field. Solid lines are fits to our model. (a) Si-GaAs at $T=280$ K; (b) InP:Fe at $T=280$ K; (c) Si-GaAs at $T=180$ K. (a)–(c) obtained with $\lambda=800$ nm pump pulses. (d) Si-GaAs at $T=180$ K measured with $\lambda=400$ nm pulses.

The authors acknowledge support from the National Science Foundation through the NSF-RUI program Contract No. DMR-0317276.

¹*Ultrafast Spectroscopy of Semiconductors and Semiconductor Nanostructures*, edited by J. Shah (Springer, Berlin, 1999), Vol. 115.

²P. G. Huggard, J. A. Cluff, G. P. Moore, C. J. Shaw, S. R. Andrews, S. R. Keiding, E. H. Linfield, and D. A. Ritchie, *J. Appl. Phys.* **87**, 2382 (2000).

³T.-I. Jeon and D. Grischkowsky, *Appl. Phys. Lett.* **72**, 3032 (1998).

⁴T.-I. Jeon and D. Grischkowsky, *Phys. Rev. Lett.* **78**, 1106 (1997).

⁵D. M. Mittleman, J. Cunningham, M. C. Nuss, and M. Geva, *Appl. Phys. Lett.* **71**, 16 (1997).

⁶M. C. Nuss, D. H. Auston, and F. Capasso, *Phys. Rev. Lett.* **58**, 2355 (1987).

⁷P. N. Saeta, J. Federici, B. I. Greene, and D. Dykaar, *Appl. Phys. Lett.* **60**, 1477 (1992).

⁸S. S. Prabhu, S. E. Ralph, M. R. Melloch, and E. S. Harmon, *Appl. Phys. Lett.* **70**, 2419 (1997).

⁹M. C. Beard, G. M. Turner, and C. A. Schmuttenmaer, *J. Phys. Chem.* **106**, 7146 (2002).

¹⁰L. Huber, F. Tauser, M. Brodschelm, M. Bichler, G. Abstreiter, and A. Leitenstorfer, *Nature (London)* **414**, 286 (2001).

¹¹K. P. H. Liu and F. A. Hegmann, *Appl. Phys. Lett.* **78**, 3478 (2001).

¹²F. A. Hegmann, T. T. Tykwinski, K. P. H. Lui, J. E. Bullock, and J. E. Anthony, *Phys. Rev. Lett.* **89**, 227403 (2002).

¹³E. Knoesel, M. Bonn, J. Shan, F. Wang, and T. F. Heinz, *J. Chem. Phys.* **121**, 394 (2004).

¹⁴V. K. Thorsmølle, R. D. Averitt, X. Chi, D. J. Hilton, D. L. Smith, A. P. Ramirez, and A. J. Taylor, *Appl. Phys. Lett.* **84**, 891 (2004).

¹⁵B. B. Hu, E. A. de Souza, W. H. Knox, J. E. Cunningham, and M. C. Nuss, *Phys. Rev. Lett.* **74**, 1689 (1995).

¹⁶J. Lloyd-Hughes, E. Castro-Camus, M. D. Fraser, C. Jagadish, and M. B. Johnston, *Phys. Rev. B* **70**, 235330 (2004).

¹⁷A. Leitenstorfer, S. Hunsche, J. Shah, M. C. Nuss, and W. H. Knox, *Phys. Rev. B* **61**, 16642 (2000).

¹⁸Polarization at $B=0$ is approximately 95% parallel to applied electric field, 5% perpendicular. We subtracted the resulting small offset from the perpendicular traces in Fig. 2.

¹⁹P. Yu and M. Cardona, *Fundamentals of Semiconductors*, 2nd ed. (Springer, New York, 1999).

²⁰Sze, *Physics of Semiconductor Devices*, 2nd ed. (Wiley, New York, 1981).

²¹M. C. Beard, G. M. Turner, and C. A. Schmuttenmaer, *Phys. Rev. B* **62**, 15764 (2000).